

# Laforin and malin knockout mice have normal glucose disposal and insulin sensitivity

Anna A. DePaoli-Roach<sup>1</sup>, Dyann M. Segvich<sup>1</sup>, Catalina M. Meyer<sup>1</sup>, Yasmeen Rahimi<sup>1</sup>, Carolyn A. Worby<sup>2</sup>, Matthew S. Gentry<sup>3</sup> and Peter J. Roach<sup>1,\*</sup>

<sup>1</sup>Department of Biochemistry and Molecular Biology, Indiana University School of Medicine, Indianapolis, IN, USA, <sup>2</sup>Department of Pharmacology, University of California, San Diego, CA, USA and <sup>3</sup>Department of Biochemistry, University of Kentucky, Lexington, KY, USA

Received October 12, 2011; Revised October 12, 2011; Accepted December 15, 2011

**Lafora disease is a fatal, progressive myoclonus epilepsy caused in ~90% of cases by mutations in the *EPM2A* or *EPM2B* genes. Characteristic of the disease is the formation of Lafora bodies, insoluble deposits containing abnormal glycogen-like material in many tissues, including neurons, muscle, heart and liver. Because glycogen is important for glucose homeostasis, the aberrant glycogen metabolism in Lafora disease might disturb whole-body glucose handling. Indeed, Vernia *et al.* [Vernia, S., Heredia, M., Criado, O., Rodriguez de Cordoba, S., Garcia-Roves, P.M., Cansell, C., Denis, R., Luquet, S., Foufelle, F., Ferre, P. *et al.* (2011) Laforin, a dual-specificity phosphatase involved in Lafora disease, regulates insulin response and whole-body energy balance in mice. *Hum. Mol. Genet.*, 20, 2571–2584] reported that *Epm2a*<sup>-/-</sup> mice had enhanced glucose disposal and insulin sensitivity, leading them to suggest that laforin, the *Epm2a* gene product, is involved in insulin signaling. We analyzed 3-month- and 6–7-month-old *Epm2a*<sup>-/-</sup> mice and observed no differences in glucose tolerance tests (GTTs) or insulin tolerance tests (ITTs) compared with wild-type mice of matched genetic background. At 3 months, *Epm2b*<sup>-/-</sup> mice also showed no differences in GTTs and ITTs. In the 6–7-month-old *Epm2a*<sup>-/-</sup> mice, there was no evidence for increased insulin stimulation of the phosphorylation of Akt, GSK-3 or S6 in skeletal muscle, liver and heart. From metabolic analyses, these animals were normal with regard to food intake, oxygen consumption, energy expenditure and respiratory exchange ratio. By dual-energy X-ray absorptiometry scan, body composition was unaltered at 3 or 6–7 months of age. Echocardiography showed no defects of cardiac function in *Epm2a*<sup>-/-</sup> or *Epm2b*<sup>-/-</sup> mice. We conclude that laforin and malin have no effect on whole-body glucose metabolism and insulin sensitivity, and that laforin is not involved in insulin signaling.**

## INTRODUCTION

Lafora disease is a fatal progressive myoclonus epilepsy, normally with onset in the teenage years followed by continued neurological decline culminating in death within 10 years (1–4). It is a genetic disease caused most frequently by mutation of either the *EPM2A* (5,6) or the *EPM2B/NHLRC1* (7) genes, which encode, respectively, laforin and malin. Laforin, by sequence, is a member of the atypical dual-specificity protein phosphatase family (5) and additionally contains a functional CBM20 carbohydrate-binding module (8).

Laforin dephosphorylates complex carbohydrates, including amylopectin (9) and glycogen (10) *in vitro*. Malin is a member of the E3 ubiquitin ligase family, and *in vitro* studies, mostly using cell systems, have suggested a number of potential targets, including laforin (11), the glycogen debranching enzyme [AGL (12)], glycogen synthase (13) and the type 1 protein phosphatase glycogen targeting subunit PTG (11,13). Of these proteins, all but laforin, have unchanged levels in *Epm2b*<sup>-/-</sup> mice (14) and it is probably fair to say that the physiological function of malin remains to be established.

\*To whom correspondence should be addressed at: Department of Biochemistry and Molecular Biology, Indiana University School of Medicine, 635 Barnhill Drive, Indianapolis, IN 46202, USA. Email: proach@iupui.edu

A consistent characteristic of Lafora disease, caused by mutation of *EPM2A* or *EPM2B*, is the accumulation of insoluble deposits called Lafora bodies in many tissues, including skeletal muscle, heart and neurons (1–4). Lafora bodies consist in large measure of polyglucosan, a branched polymer of glucose that resembles the normal storage compound glycogen in containing glucose residues linked by  $\alpha$ -1,4- and  $\alpha$ -1,6-glycosidic linkages. Polyglucosan, however, contains fewer  $\alpha$ -1,6 branch points than glycogen, making it less branched, less soluble and more like the amylopectin found in plant starch (15). Lafora bodies in Lafora patients (16) and glycogen in *Epm2a*<sup>-/-</sup> (10,17) and *Epm2b*<sup>-/-</sup> (18) mice also contain elevated levels of covalent phosphate, a normal trace constituent of glycogen (19). For the laforin knockout animals, this result supports the hypothesis that laforin dephosphorylates glycogen *in vivo* (10). Increased glycogen phosphorylation is associated with disturbances in glycogen structure that are consistent with Lafora body formation (17). Lafora bodies appear to be linked to the pathology of the disease since reduction of their formation by genetically eliminating PTG in an *Epm2a*<sup>-/-</sup> background ameliorated neurological symptoms in mice (20). Therefore, there is emerging evidence that Lafora disease can be viewed as a non-classical glycogenosis.

Given the association between laforin and abnormal glycogen metabolism in *Epm2a*<sup>-/-</sup> mice, one could postulate that glucose homeostasis might be disturbed in these animals. In fact, Vernia *et al.* (21) recently reported that 3-month-old *Epm2a*<sup>-/-</sup> mice had altered metabolism and insulin sensitivity. In their study, the *Epm2a*<sup>-/-</sup> animals were heavier, had higher adiposity and had increased food intake. Paradoxically, they were hypoglycemic and, compared with wild-type mice, displayed a major improvement in glucose disposal during a glucose tolerance test (GTT) and were more insulin-sensitive as judged by insulin tolerance tests (ITTs). From calorimetric analyses, the *Epm2a*<sup>-/-</sup> mice had increased oxygen consumption, energy expenditure and respiratory exchange ratio (RER). In addition, insulin-stimulated phosphorylation of downstream signaling targets, including Akt and GSK-3, was greater in the *Epm2a*<sup>-/-</sup> mice, especially in the heart. Based on their results, Vernia *et al.* (21) proposed that laforin is a novel component of the insulin signaling pathway, a finding that would have broad implications both for the mechanism of insulin action and for Lafora disease.

To explore this hypothesis further, we compared metabolic parameters in *Epm2a*<sup>-/-</sup> and wild-type control mice in a matched genetic background at 3 months and 6–7 months of age. We found no statistically significant differences in glucose disposal as assessed by GTTs or whole-body insulin sensitivity as monitored by ITTs. Analyses of downstream molecular markers of insulin action in muscle, liver and heart likewise revealed no differences between the genotypes. We additionally analyzed 3-month-old *Epm2b*<sup>-/-</sup> mice and wild-type controls and observed no change in either GTTs or ITTs. Echocardiography analyses of *Epm2a*<sup>-/-</sup> and *Epm2b*<sup>-/-</sup> mice showed no defects in cardiac function. Our data do not provide any evidence for a role of Lafora genes in determining insulin sensitivity or insulin signaling in mice.

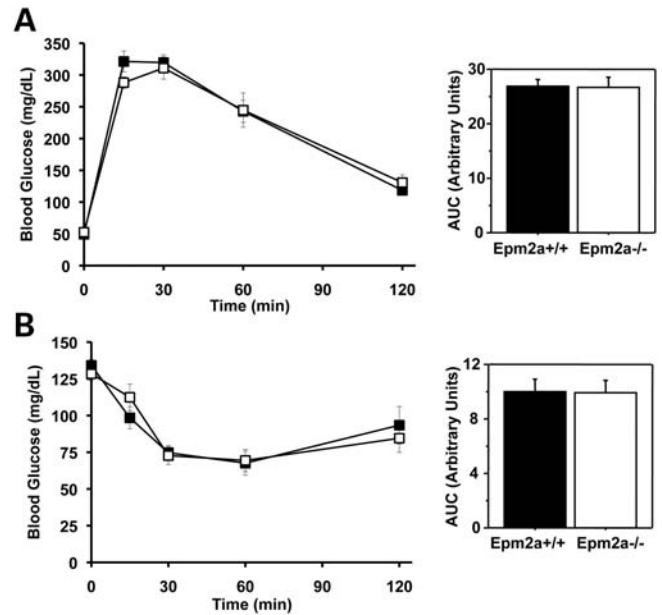


**Figure 1.** Glucose disposal and insulin sensitivity of *Epm2a*<sup>-/-</sup> mice. Male wild-type mice (filled symbols) and *Epm2a*<sup>-/-</sup> mice (open symbols), 6–7 months of age, were analyzed by GTTs (A) and ITTs (B) as described under Materials and Methods. The bar graphs report AUCs. Shown are the means and standard errors of the mean. Wild-type, *n* = 7; *Epm2a*<sup>-/-</sup>, *n* = 7.

**Table 1.** Weight, body composition and blood glucose levels of 6–7-month-old male *Epm2a*<sup>-/-</sup> mice

	<i>Epm2a</i> <sup>+/+</sup>	<i>Epm2a</i> <sup>-/-</sup>
Number of mice ( <i>n</i> )	7	7
Weight (g)	31.7 ± 0.9	32.5 ± 0.6
Fed blood glucose (mg/dl)	133 ± 4	128 ± 4
Fasted blood glucose (mg/dl)	49 ± 2	53 ± 3
Fat mass (%)	25.3 ± 2.1	22.8 ± 2.4
Lean mass (%)	74.7 ± 2.1	77.2 ± 2.4

## RESULTS

### Metabolic analyses of *Epm2a*<sup>-/-</sup> mice

Laforin knockout and wild-type control mice, 6–7 months of age, were analyzed by intraperitoneal GTT (Fig. 1). The blood glucose levels were similar between genotypes, from the starting fasting value through the course of the experiment, as is reflected in the unchanged values for the area under the curve (AUC). The same groups of animals, after resting for 1 week, were subjected to intraperitoneal ITTs. Again, the data for the two genotypes were statistically indistinguishable (Fig 1). The two groups of mice had identical weights, body composition as judged by dual-energy X-ray absorptiometry (DEXA) scan, and fed and fasted blood glucose levels (Table 1).

To further explore whole-body metabolism in the *Epm2a*<sup>-/-</sup> mice, we analyzed them by indirect calorimetry in metabolic cages. After acclimatization to the cages, the animals were monitored for 36 h with food, 24 h without food and then 24 h after refeeding. The charts for oxygen

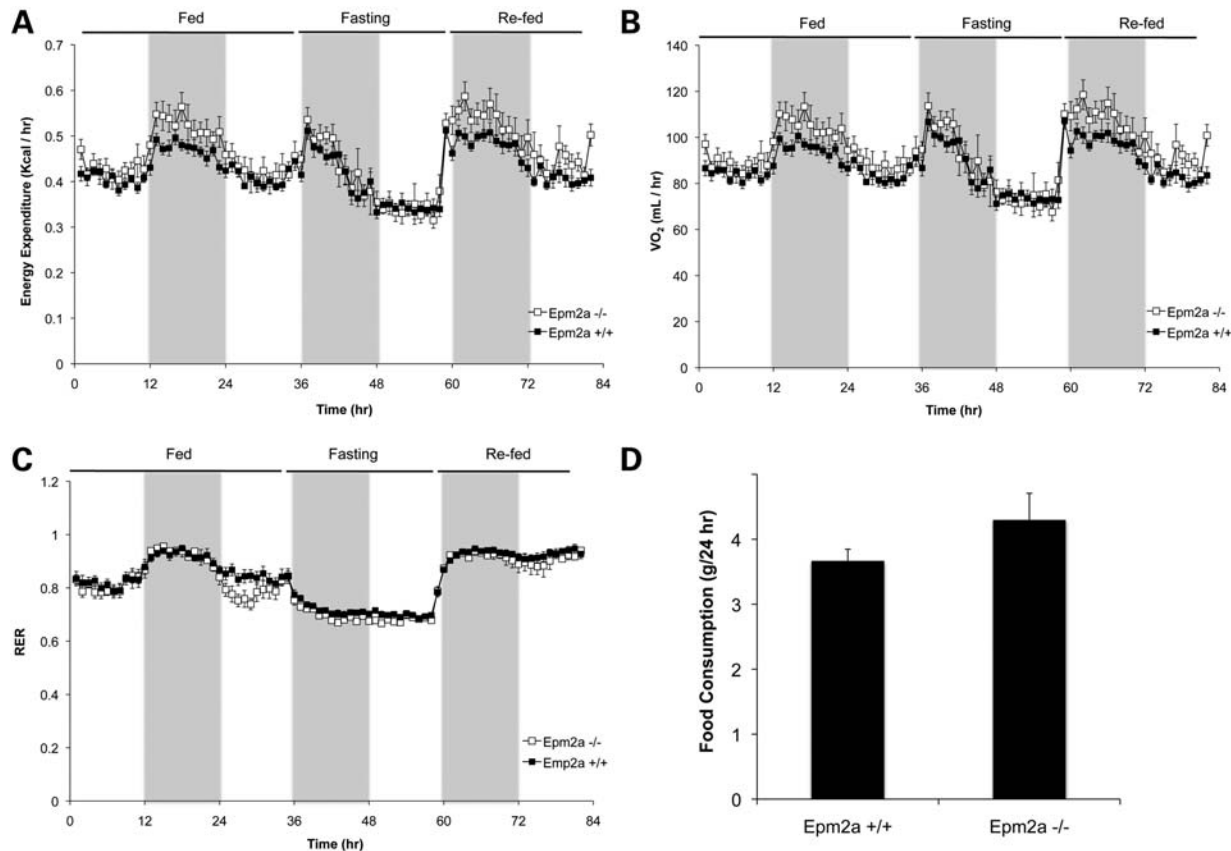


**Figure 2.** Indirect calorimetry and food consumption of *Epm2a*<sup>-/-</sup> mice. Male wild-type mice (filled symbols) and *Epm2a*<sup>-/-</sup> mice (open symbols) were analyzed in metabolic cages to monitor energy expenditure (A), oxygen consumption ( $VO_2$ ; B) and RER (C). The shaded areas correspond to the 12 h dark cycles. Food consumption (D) was measured over a 24 h period. Shown are the means and standard errors of the mean. Wild-type,  $n = 7$ ; *Epm2a*<sup>-/-</sup>,  $n = 5$ .

consumption,  $CO_2$  production, energy expenditure and RER were largely overlapping (Fig. 2 and Supplementary Material, Fig. S1). To enable better statistical comparisons, for each mouse, the AUC was calculated for each 12 h light or dark cycle over the whole experiment (Supplementary Material, Fig. S1). There were no statistically significant differences between genotypes except for a small difference over one 12 h period. Our conclusion from these analyses is that the *Epm2a*<sup>-/-</sup> mice were essentially indistinguishable from wild-type animals. The same experiment also allowed monitoring of food consumption (Fig. 2D) and locomotor activity (not shown), which were not statistically different between *Epm2a*<sup>-/-</sup> and wild-type mice.

### Insulin signaling pathway in *Epm2a*<sup>-/-</sup> mice

To assess insulin signaling, mice were treated by intraperitoneal injection of insulin, reducing the blood glucose by ~50% compared with injection of vehicle and demonstrating that the insulin had functioned (Fig. 3B). Consistent with the ITT data, there was no difference in the degree of reduction of blood glucose between *Epm2a*<sup>-/-</sup> and wild-type mice (Fig. 3B). Skeletal muscle, liver and heart were harvested after 10 min for analysis of downstream targets of insulin signaling by western blotting with phospho-specific antibodies. In muscle from wild-type mice, the phosphorylation of Akt

(Thr308 and Ser473), GSK-3 $\alpha$  (Ser21) and GSK-3 $\beta$  (Ser9), TSC2 (Thr1462) and S6 (Ser235/236) was increased and phosphorylation of glycogen synthase site 3a was decreased by insulin, all as expected (Fig. 3). Statistically indistinguishable results were observed with *Epm2a*<sup>-/-</sup> animals treated with insulin. In the liver, insulin increased phosphorylation of the same downstream targets in wild-type mice (Supplementary Material, Fig. S2). In the liver, as in muscle, there were no indications of altered insulin signaling in the *Epm2a*<sup>-/-</sup> mice when compared with wild-type. It has been suggested that laforin may act upstream of TSC2 to control the mTor pathway and possibly autophagy (22). The lack of differences in the phosphorylation of TSC2 at T1462, a site phosphorylated by Akt, in muscle and liver indicates that laforin is not involved in the dephosphorylation of this site. In the heart, insulin-stimulated phosphorylation of Akt, GSK-3 $\alpha$ , GSK-3 $\beta$  and S6 was also unaffected by the absence of laforin in the *Epm2a*<sup>-/-</sup> mice (Supplementary Material, Fig. S3).

### Glucose disposal and insulin sensitivity in 3-month-old *Epm2a*<sup>-/-</sup> and *Epm2b*<sup>-/-</sup> mice

Since Vernia *et al.* (21) analyzed younger mice (3 months old) in their study, we repeated key experiments with mice of a comparable age. Even at this young age, Lafora bodies have

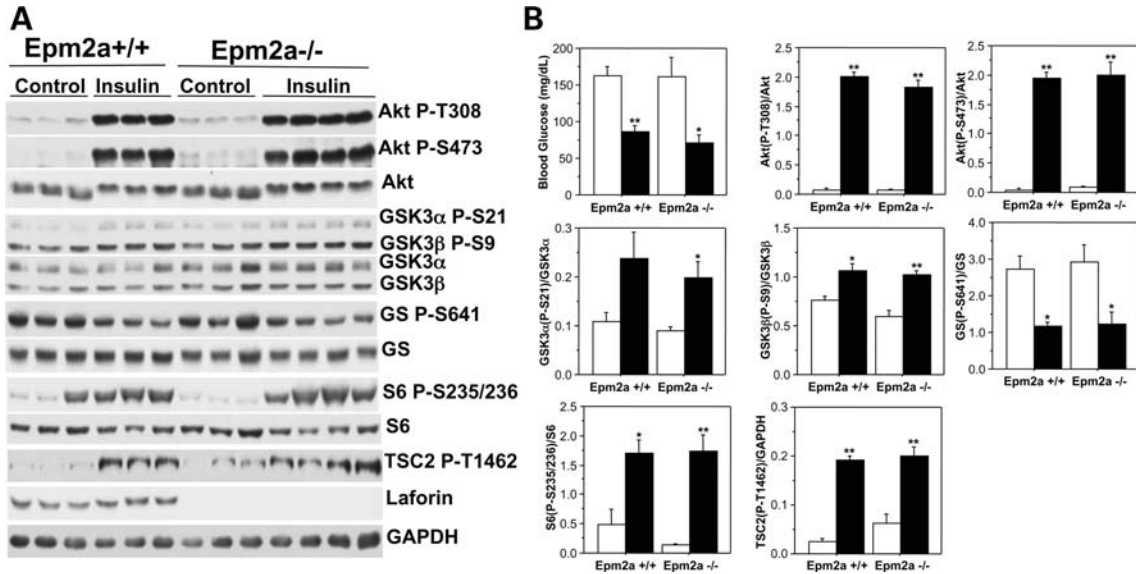


**Figure 3.** Insulin signaling in skeletal muscle of *Epm2a*<sup>-/-</sup> mice. Insulin or vehicle was administered intraperitoneally to 6–7-month-old wild-type and *Epm2a*<sup>-/-</sup> mice, as indicated. After 10 min, blood glucose was analyzed (**B**) and tissues harvested for analysis. Skeletal muscle was processed as described under Materials and Methods and analyzed by western blotting (**A**) using the indicated antibodies. Quantitation of western blots (**B**) compares phosphorylation normalized by total protein (in arbitrary units) for vehicle-treated (open bars) and insulin-treated mice (solid bars) of each genotype. Shown are the means and standard errors of the mean. Wild-type, vehicle, *n* = 3; wild-type, insulin, *n* = 3; *Epm2a*<sup>-/-</sup>, vehicle, *n* = 3; *Epm2a*<sup>-/-</sup>, insulin, *n* = 4. \**P* < 0.05 with respect to control; \*\**P* < 0.01 with respect to control.

begun to accumulate in several tissues of both *Epm2a*<sup>-/-</sup> (23) and *Epm2b*<sup>-/-</sup> (14) mice. The experimental animal groups at this age did not differ in fed or fasting blood glucose, body composition or weight (Supplementary Material, Table S1). When subjected to a GTT, the *Epm2a*<sup>-/-</sup> mice responded identically to wild-type controls (Supplementary Material, Fig. S4). Likewise, the *Epm2a*<sup>-/-</sup> mice displayed similar insulin sensitivity judged by ITTs (Supplementary Material, Fig. S4). *Epm2b*<sup>-/-</sup> mice of the same age were analyzed similarly and in these animals, the absence of malin had no effect on either glucose disposal as judged by GTT or insulin sensitivity as monitored by ITTs (Fig. 4).

#### Analysis of cardiac function in *Epm2a*<sup>-/-</sup> mice

Vernia *et al.* (21) reported that insulin signaling was strongly enhanced in the hearts of *Epm2a*<sup>-/-</sup> mice. In addition, the heart is especially prone to the development of Lafora bodies in *Epm2b*<sup>-/-</sup> mice (14). Furthermore, several other glycogenoses severely impact the heart, including Pompe disease (24,25), Danon disease (26) and *PRKAG2* mutation often linked to Wolff–Parkinson–White syndrome (27,28). Therefore, we analyzed wild-type, *Epm2a*<sup>-/-</sup> and *Epm2b*<sup>-/-</sup> mice by echocardiography, both before and after administration of isoproterenol for 5 min. As expected, isoproterenol increased heart rate and ejection fraction with concomitant decreases in left ventricular diameters and volumes. None of the parameters measured in the knockout animals, before or after isoproterenol administration, differed significantly from wild-type controls (Supplementary Material, Table S2).

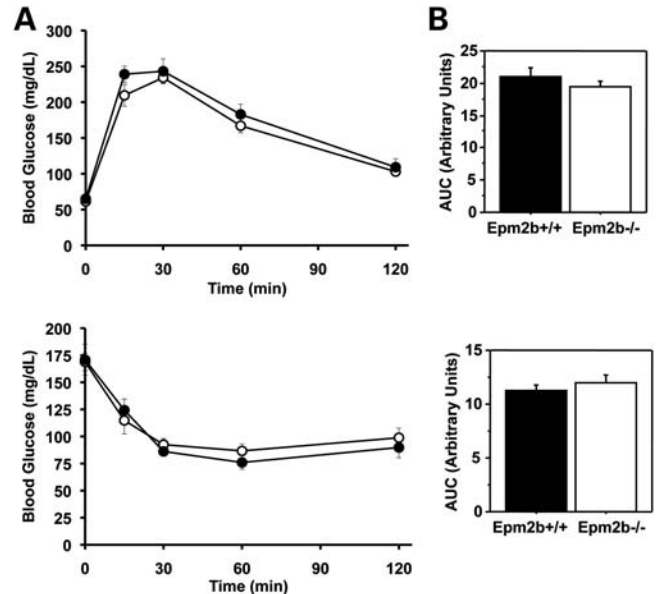


**Figure 4.** Glucose disposal and insulin sensitivity of *Epm2b*<sup>-/-</sup> mice. Male wild-type mice (filled symbols) and *Epm2b*<sup>-/-</sup> mice (open symbols), 3 months of age, were analyzed by GTTs (**A**) and ITTs (**B**) as described under Materials and Methods. The bar graphs report AUCs. Shown are the means and standard errors of the mean. Wild-type, *n* = 6; *Epm2b*<sup>-/-</sup>, *n* = 6.

## DISCUSSION

Since mutations of the *EPM2A* and *EPM2B* genes correlate with deposition of abnormal glycogen in major organs, it is not unreasonable to hypothesize that glucose homeostasis might be disturbed. The literature on Lafora patients does

not describe alterations in glucose metabolism but enhanced glucose handling might not have surfaced given the more pressing clinical symptoms of these patients. In an effort to replicate and possibly extend the work of Vernia *et al.* (21), we analyzed *Epm2a*<sup>-/-</sup> mice, and to a lesser extent *Epm2b*<sup>-/-</sup> mice, for glucose metabolism and insulin signaling.

In all the biochemical and physiological tests applied, we observed virtually no statistically significant differences between *Epm2a*<sup>-/-</sup> mice and wild-type controls. Most importantly, neither 3-month-old nor 6–7-month-old animals displayed differences in glucose disposal as judged by GTT and insulin sensitivity as assessed by ITTs. At 6–7 months of age, we found no changes in the activation of downstream intracellular targets of insulin action in muscle, liver or heart. Other whole-body measures of metabolic activity, including oxygen consumption, energy expenditure and RER, were identical between genotypes as was lean or fat weight measured by DEXA scan. Our more limited study of 3-month-old *Epm2b*<sup>-/-</sup> mice did not indicate any changes in glucose disposal or insulin sensitivity.

Our results contrast with many of those reported by Vernia *et al.* (21) and the reason for the difference is not wholly clear. Many factors can influence experiments with animals, including diet, environment and housing, and genetic backgrounds. The wild-type and *Epm2a*<sup>-/-</sup> mice used in our study had matched genetic backgrounds and were bred in parallel in our colony (see Materials and Methods). Vernia *et al.* (21) obtained *Epm2a*<sup>-/-</sup> mice from Dr Delgado-Escueta, citing the original report of Ganesh *et al.* (23), which described the mice as having a mixed C57BL/6 × 129Svj background. They used C57BL/6 mice from Jackson Laboratories as wild-type controls. The C57BL/6 strain is known to be relatively insulin-insensitive compared with 129 strains, for example when analyzed by a GTT (29). Whether or not genetic background differences contribute to the discrepant results, our work constitutes an independent study indicating that glucose disposal and insulin sensitivity are normal in mice lacking laforin or malin.

## MATERIALS AND METHODS

### Mouse models

*Epm2a*<sup>-/-</sup> mice in a mixed C57BL/6 × 129Svj background (23) were obtained from Dr Delgado-Escueta and backcrossed five times with C57BL/6 mice. Heterozygotes from this generation were crossed to generate *Epm2a*<sup>-/-</sup> and *Epm2a*<sup>+/+</sup> mice. Intercrossing of these mice (*Epm2a*<sup>-/-</sup> × *Epm2a*<sup>-/-</sup> and *Epm2a*<sup>+/+</sup> × *Epm2a*<sup>+/+</sup>) produced the experimental mice used in this study. *Epm2b*<sup>-/-</sup> mice were generated as described by DePaoli-Roach *et al.* (14). Briefly, C57BL/6 ES cells disrupted for *Epm2b* were injected into C57BL/6 blastocysts, which resulted in a male chimeric mouse that gave germline transmission after crossing with C57BL/6 females. The resulting *Epm2b*<sup>-/+</sup> mice were intercrossed and the resulting progeny used for *Epm2b*<sup>-/-</sup> × *Epm2b*<sup>-/-</sup> and *Epm2b*<sup>+/+</sup> × *Epm2b*<sup>+/+</sup> crosses to generate the experimental animals. All experiments utilized the indicated numbers of male mice. All mice were

maintained in temperature- and humidity-controlled conditions with 12:12 h light–dark cycle at the Indiana University School of Medicine Laboratory Animal Resource Center, were fed a standard chow (Harlan Teklad global diet 2018SX) and allowed food and water *ad libitum* unless indicated. All studies were conducted in accordance with federal guidelines and were approved by the Institutional Animal Care and Use Committee of Indiana University School of Medicine.

### GTTs and ITTs

GTTs and ITTs were performed on 6–7-month-old male wild-type and *Epm2a*<sup>-/-</sup> mice as well as on 3-month-old *Epm2a*<sup>-/-</sup> and *Epm2b*<sup>-/-</sup> mice together with wild-type animals of the corresponding genetic background. For GTTs, animals were fasted for 16 h and injected intraperitoneally with a 20% sterile glucose solution in H<sub>2</sub>O to a final dose of 2 g/kg body weight. Blood glucose was monitored at 0, 15, 30, 60 and 120 min by a tail snip using a Contour Glucometer (Bayer). For ITTs, 5 h fasted animals (from 8:30 a.m. to 1:30 p.m.) were injected intraperitoneally with 0.75 U/kg HumulinR (Eli Lilly and Co.) in sterile saline. Blood glucose was monitored as for the GTT.

### Calorimetric analyses

RER, energy expenditure, food consumption and motor activity were measured in 6–7-month-old male *Epm2a* knockout and wild-type control mice with an Animal Monitoring System (Lab Master, TSE systems, Midland, MI, USA). The system consists of an eight-cage open-circuit system equipped with an air pump, a control unit, a sample switch unit to draw air samples from the cages and an air-drying unit. After 48 h acclimation in the calorimetric cages, the mice were recorded for 36 h for the measurements listed above. Subsequently, food but not water was removed for 24 h followed by 24 h refeeding. The system measures oxygen consumed and carbon dioxide produced; RER was calculated as the ratio of carbon dioxide produced divided by oxygen consumed. These values were averaged to determine the hourly rate of each parameter. Energy expenditure was calculated by the Weir equation (30) as modified by Bruss *et al.* (31): Energy expenditure (kcal/h) = [(3.815 + 1.232 × RER) × VO<sub>2</sub>]/1000, where VO<sub>2</sub> is in milliliters/hour.

### Body composition

Fat mass and lean body mass of wild-type and *Epm2a*<sup>-/-</sup> mice were estimated by DEXA scanning. A PIXImus II mouse densitometer (Lunar Corp., Madison, WI, USA) was used in the Department of Cell Biology and Anatomy, Indiana University School of Medicine. During scanning, the mice were maintained in the anesthetized state by a constant flow of isoflurane gas (2% with oxygen at a rate of 1 l/min) administered by a nose cone. The duration of the scan was 4–5 min.

### Insulin signaling and western blotting

For the assessment of insulin signaling, awake 6–7-month-old male *Epm2a*<sup>-/-</sup> and wild-type mice fasted for ~4–5 h (8:30 a.m.–1:30 p.m.) were injected intraperitoneally with 5 mU/g HumulinR or vehicle. After 10 min, blood glucose was measured and animals were sacrificed by cervical dislocation followed by decapitation. Skeletal muscle, liver and heart were immediately frozen in liquid nitrogen and stored at –80°C until use. Liquid-nitrogen-powdered tissue samples were homogenized in 15 volumes of ice-cold buffer (50 mM Tris–HCl, pH 7.8, 10 mM EDTA, 2 mM EGTA, 100 mM NaF, 2 mM benzamide, 0.1 mM N $\alpha$ -*p*-tosyl-L-lysine chloromethyl ketone, 50 mM  $\beta$ -mercaptoethanol, 0.5 mM PMSF, 10  $\mu$ g/ml leupeptin, 1 mM sodium orthovanadate and 0.2% Triton X-100) using a Tissue Tearer Model 985–370 (Biospec Products, Inc.) at maximal speed for 20–30 s. The homogenates were centrifuged at 6500g for 10 min and the supernatant used for western blot analyses. Either 10 or 30  $\mu$ g of protein were analyzed by 10% SDS–PAGE. After transfer, the nitrocellulose membranes were stained with Ponceau S to monitor loading, followed by blocking in TBS-T containing 5% non-fat milk for 1 h. Blots were probed with various antibodies in TBS-T plus 2% non-fat milk, which included: anti-Akt, anti-phospho Akt(Thr308), anti-phospho-Akt (Ser473), anti-phospho GSK3 (Ser9/21), anti-glycogen synthase, anti-phospho glycogen synthase (Ser641-phospho-site 3a), anti-S6, anti-phospho S6 (Ser235/236) and anti-phospho TSC2 (Thr1462) from Cell Signaling Technology, anti-GSK-3 from Invitrogen Corporation, anti-laforin from Abnova and anti-GAPDH from Biodesign International. Detection was performed by enhanced chemiluminescence followed by autoradiography. The levels of protein expression were quantitated by densitometric scanning of the autoradiograms.

### Heart function

Cardiac dimensions and contractility of 7–8-month-old male wild-type, *Epm2a*<sup>-/-</sup> and *Epm2b*<sup>-/-</sup> mice were evaluated by noninvasive transthoracic echocardiography with a Vevo 770 High Resolution Imaging System (VisualSonics, Inc., Toronto, Canada) at the Indiana Center for Vascular Biology and Medicine. Mice were anesthetized by inhaling isoflurane (2% via nose cone) and maintained on a platform at 37°C during ultrasound scanning with a 35 MHz mechanical transducer. Mice were scanned before and 5 min after intraperitoneal injection of isoproterenol (100 ng/g body weight). Left ventricular chamber dimension and wall thickness were measured from M-mode recordings. Heart rate and EKG were also monitored simultaneously. Fractional shortening was calculated from left ventricular end-systolic and end-diastolic dimensions using the formula: (LVEDD – LVESD)/LVEDD  $\times$  100.

### Statistical analyses

The data are presented as the mean  $\pm$  SEM of the indicated number of animals. Statistical significance was evaluated by

an unpaired Student's *t*-test and was considered significant at  $P < 0.05$ .

### SUPPLEMENTARY MATERIAL

Supplementary Material is available at *HMG* online.

### ACKNOWLEDGEMENTS

We acknowledge Dr Mark Payne and Mr Todd Cook for help with the echocardiography.

*Conflict of Interest statement.* None declared.

### FUNDING

This work was supported by NIH grants DK27221 (P.J.R.), NS056454 (P.J.R.) NS061803 (M.S.G.), NS070899 (M.S.G.), DK18024 (C.A.W.) and DK018849 (C.A.W.).

### REFERENCES

- Ramachandran, N., Girard, J.M., Turnbull, J. and Minassian, B.A. (2009) The autosomal recessively inherited progressive myoclonus epilepsies and their genes. *Epilepsia*, **50** (Suppl. 5), 29–36.
- Gentry, M.S., Dixon, J.E. and Worby, C.A. (2009) Lafora disease: insights into neurodegeneration from plant metabolism. *Trends Biochem. Sci.*, **34**, 628–639.
- Delgado-Escueta, A.V. (2007) Advances in Lafora progressive myoclonus epilepsy. *Curr. Neurol. Neurosci. Rep.*, **7**, 428–433.
- Ganesh, S., Puri, R., Singh, S., Mittal, S. and Dubey, D. (2006) Recent advances in the molecular basis of Lafora's progressive myoclonus epilepsy. *J. Hum. Genet.*, **51**, 1–8.
- Minassian, B.A., Lee, J.R., Herbrick, J.A., Huizenga, J., Soder, S., Mungall, A.J., Dunham, I., Gardner, R., Fong, C.Y., Carpenter, S. *et al.* (1998) Mutations in a gene encoding a novel protein tyrosine phosphatase cause progressive myoclonus epilepsy. *Nat. Genet.*, **20**, 171–174.
- Serratosa, J.M., Gomez-Garre, P., Gallardo, M.E., Anta, B., de Bernabe, D.B., Lindhout, D., Augustijn, P.B., Tassinari, C.A., Malafosse, R.M., Topcu, M. *et al.* (1999) A novel protein tyrosine phosphatase gene is mutated in progressive myoclonus epilepsy of the Lafora type (EPM2). *Hum. Mol. Genet.*, **8**, 345–352.
- Chan, E.M., Young, E.J., Ianzano, L., Munteanu, I., Zhao, X., Christopoulos, C.C., Avanzini, G., Elia, M., Ackerley, C.A., Jovic, N.J. *et al.* (2003) Mutations in NHLRC1 cause progressive myoclonus epilepsy. *Nat. Genet.*, **35**, 125–127.
- Wang, J., Stuckey, J.A., Wishart, M.J. and Dixon, J.E. (2002) A unique carbohydrate binding domain targets the Lafora disease phosphatase to glycogen. *J. Biol. Chem.*, **277**, 2377–2380.
- Worby, C.A., Gentry, M.S. and Dixon, J.E. (2006) Laforin: a dual specificity phosphatase that dephosphorylates complex carbohydrates. *J. Biol. Chem.*, **281**, 30412–30418.
- Tagliabracci, V.S., Turnbull, J., Wang, W., Girard, J.M., Zhao, X., Skurat, A.V., Delgado-Escueta, A.V., Minassian, B.A., Depaoli-Roach, A.A. and Roach, P.J. (2007) Laforin is a glycogen phosphatase, deficiency of which leads to elevated phosphorylation of glycogen in vivo. *Proc. Natl Acad. Sci. USA*, **104**, 19262–19266.
- Worby, C.A., Gentry, M.S. and Dixon, J.E. (2008) Malin decreases glycogen accumulation by promoting the degradation of protein targeting to glycogen (PTG). *J. Biol. Chem.*, **283**, 4069–4076.
- Cheng, A., Zhang, M., Gentry, M.S., Worby, C.A., Dixon, J.E. and Saltiel, A.R. (2007) A role for AGL ubiquitination in the glycogen storage disorders of Lafora and Cori's disease. *Genes Dev.*, **21**, 2399–2409.
- Vilchez, D., Ros, S., Cifuentes, D., Pujadas, L., Valles, J., Garcia-Fojeda, B., Criado-Garcia, O., Fernandez-Sanchez, E., Medrano-Fernandez, I., Dominguez, J. *et al.* (2007) Mechanism suppressing glycogen synthesis in

- neurons and its demise in progressive myoclonus epilepsy. *Nat. Neurosci.*, **10**, 1407–1413.
14. DePaoli-Roach, A.A., Tagliabracci, V.S., Segvich, D.M., Meyer, C.M., Irimia, J.M. and Roach, P.J. (2010) Genetic depletion of the malin E3 ubiquitin ligase in mice leads to Lafora bodies and the accumulation of insoluble laforin. *J. Biol. Chem.*, **285**, 25372–25381.
  15. Ball, S., Guan, H.P., James, M., Myers, A., Keeling, P., Mouille, G., Buleon, A., Colonna, P. and Preiss, J. (1996) From glycogen to amylopectin: a model for the biogenesis of the plant starch granule. *Cell*, **86**, 349–352.
  16. Sakai, M., Austin, J., Witmer, F. and Trueb, L. (1970) Studies in myoclonus epilepsy (Lafora body form). II. Polyglucosans in the systemic deposits of myoclonus epilepsy and in corpora amylacea. *Neurology*, **20**, 160–176.
  17. Tagliabracci, V.S., Girard, J.M., Segvich, D., Meyer, C., Turnbull, J., Zhao, X., Minassian, B.A., Depaoli-Roach, A.A. and Roach, P.J. (2008) Abnormal metabolism of glycogen phosphate as a cause for Lafora disease. *J. Biol. Chem.*, **283**, 33816–33825.
  18. Turnbull, J., Wang, P., Girard, J.M., Ruggieri, A., Wang, T.J., Draginov, A.G., Kameka, A.P., Pencea, N., Zhao, X., Ackerley, C.A. *et al.* (2010) Glycogen hyperphosphorylation underlies Lafora body formation. *Ann. Neurol.*, **68**, 925–933.
  19. Fontana, J.D. (1980) The presence of phosphate in glycogen. *FEBS Lett.*, **109**, 85–92.
  20. Turnbull, J., Depaoli-Roach, A.A., Zhao, X., Cortez, M.A., Pencea, N., Tiberia, E., Piliguiian, M., Roach, P.J., Wang, P., Ackerley, C.A. *et al.* (2011) PTG depletion removes Lafora bodies and rescues the fatal epilepsy of Lafora disease. *PLoS Genet.*, **7**, e1002037.
  21. Vernia, S., Heredia, M., Criado, O., Rodriguez de Cordoba, S., Garcia-Roves, P.M., Cansell, C., Denis, R., Luquet, S., Fougelle, F., Ferre, P. *et al.* (2011) Laforin, a dual specificity phosphatase involved in Lafora disease, regulates insulin response and whole-body energy balance in mice. *Hum. Mol. Genet.*, **20**, 2571–2584.
  22. Aguado, C., Sarkar, S., Korolchuk, V.I., Criado, O., Vernia, S., Boya, P., Sanz, P., de Cordoba, S.R., Knecht, E. and Rubinsztein, D.C. (2010) Laforin, the most common protein mutated in Lafora disease, regulates autophagy. *Hum. Mol. Genet.*, **19**, 2867–2876.
  23. Ganesh, S., Delgado-Escueta, A.V., Sakamoto, T., Avila, M.R., Machado-Salas, J., Hoshii, Y., Akagi, T., Gomi, H., Suzuki, T., Amano, K. *et al.* (2002) Targeted disruption of the Epm2a gene causes formation of Lafora inclusion bodies, neurodegeneration, ataxia, myoclonus epilepsy and impaired behavioral response in mice. *Hum. Mol. Genet.*, **11**, 1251–1262.
  24. Raben, N., Plotz, P. and Byrne, B.J. (2002) Acid alpha-glucosidase deficiency (glycogenosis type II, Pompe disease). *Curr. Mol. Med.*, **2**, 145–166.
  25. Reuser, A.J., Kroos, M.A., Hermans, M.M., Bijvoet, A.G., Verbeet, M.P., Van Diggelen, O.P., Kleijer, W.J. and Van der Ploeg, A.T. (1995) Glycogenosis type II (acid maltase deficiency). *Muscle Nerve*, **3**, S61–S69.
  26. Danon, M.J., Oh, S.J., DiMauro, S., Manaligod, J.R., Eastwood, A., Naidu, S. and Schliselfeld, L.H. (1981) Lysosomal glycogen storage disease with normal acid maltase. *Neurology*, **31**, 51–57.
  27. Arad, M., Seidman, C.E. and Seidman, J.G. (2007) AMP-activated protein kinase in the heart: role during health and disease. *Circ. Res.*, **100**, 474–488.
  28. Kim, A.S., Miller, E.J. and Young, L.H. (2009) AMP-activated protein kinase: a core signalling pathway in the heart. *Acta Physiol. (Oxf.)*, **196**, 37–53.
  29. Goren, H.J., Kulkarni, R.N. and Kahn, C.R. (2004) Glucose homeostasis and tissue transcript content of insulin signaling intermediates in four inbred strains of mice: C57BL/6, C57BLKS/6, DBA/2, and 129X1. *Endocrinology*, **145**, 3307–3323.
  30. Weir, J.B. (1949) New methods for calculating metabolic rate with special reference to protein metabolism. *J. Physiol.*, **109**, 1–9.
  31. Bruss, M.D., Khambatta, C.F., Ruby, M.A., Aggarwal, I. and Hellerstein, M.K. (2010) Calorie restriction increases fatty acid synthesis and whole body fat oxidation rates. *Am. J. Physiol. Endocrinol. Metab.*, **298**, E108–E116.